

This is the peer reviewed version of the following article: Adv. Mater. Interfaces 2015, 2, 1500323, which has been published in final form at <https://onlinelibrary.wiley.com/doi/full/10.1002/admi.201500323>. This article may be used for non-commercial purposes in accordance with Wiley Terms and Conditions for Use of Self-Archived Versions.

Article type: Full Paper

Tuning the electronic structure of graphene through collective electrostatic effects

*Gernot J. Kraberger, David A. Egger, Egbert Zojer**

Gernot J. Kraberger, Dr. David Egger, Prof. Egbert Zojer
Institute of Solid State Physics, NAWI Graz, Graz University of Technology, Petersgasse 16,
8010 Graz, Austria
E-mail: egbert.zojer@tugraz.at

Dr. David A. Egger
Present Address: Department of Materials and Interfaces, Weizmann Institute of Science,
Rehovoth 76100, Israel.

Keywords: graphene; 2D materials; DFT calculations; collective electrostatic effects; orbital localization

Electrostatically designing materials opens a new avenue for realizing systems with user-defined electronic properties. Here, an approach is presented for efficiently patterning the electronic structure of layered systems such as graphene by means of collective electrostatic effects. Using density-functional theory simulations, it is found that lines of polar elements can strongly modify the energy landscape of this prototypical 2D material. This results in a confinement of electronic states in specific regions of the sample and, consequently, in a local energetic shifting of the density of states. The latter is also directly reflected in the details in the band-structure of the electrostatically patterned sample. Finally, it is shown that our approach can be successfully applied also to other 2D materials such as hexagonal boron nitride, where the effects are predicted to be even more pronounced than in graphene.

1. Introduction

One of the most fascinating prospects of graphene is the possibility to use it as part of novel electronic devices^[1,2]. It is particularly suited for miniaturization purposes and for high frequency applications^[3-6], as it is atomically thin and has a very high electron mobility. Moreover, these properties allow its application as electrode material in thin-film transistors that are entirely composed of 2D materials^[7-9]. For more complex applications involving graphene it is highly desirable to modify its electronic properties in a controlled manner. For example, with B^[10,11] and N^[12-15] atoms that are substituted into the graphene structure it is possible to tune the position of the Fermi-level in graphene relative to the Dirac-cone in its band structure. Furthermore, chemical modification of graphene either through hydrogenation^[16] or fluorination^[17] also allows opening a larger band-gap, which is one prerequisite for using it as the active material in logical devices^[18]. Beyond modifying graphene on a rather “macroscopic” scale, it is also desirable to tune its electronic structure more locally, in particular confining electronic states spatially and controlling their energies. This may eventually enable a local patterning of paths in which charge-carriers flow and could, thus, enable the application of graphene in more complex electrical circuits. In this contribution we propose a general strategy for achieving pronounced localization and energetic control of the electronic states of graphene by means of collective electrostatic effects.

These effects arise from the superposition of the fields of a large number of dipoles that are arranged in an ordered fashion. Conceptually, one has to distinguish between 2D- and 1D-assemblies of dipoles. Specifically, a 2D-array of dipoles arranged in a plane with dipole moments perpendicular to that plane causes a rigid shift of the electrostatic energies between either sides of the assembly, as schematically shown in **Figure 1a**. Such 2D electrostatic effects are highly relevant for understanding the electronic properties of organic/inorganic

interfaces^[19], in particular for self-assembled monolayers adsorbed on semiconductors^[20] and metals^[21], and were recently suggested as means to realize organic monolayer quantum-wells and cascades^[22]. For modifying the properties of materials that are intrinsically 2D such as, e.g., graphene, monolayers of hexagonal BN, or layered semiconductors, we here propose to use 1D-lines of dipoles. For such a dipole line, the electrostatic potential is not constant left and right of the dipole assembly, but rather falls off to zero according to a $1/\text{distance}$ law as schematically shown in Figure 1b.

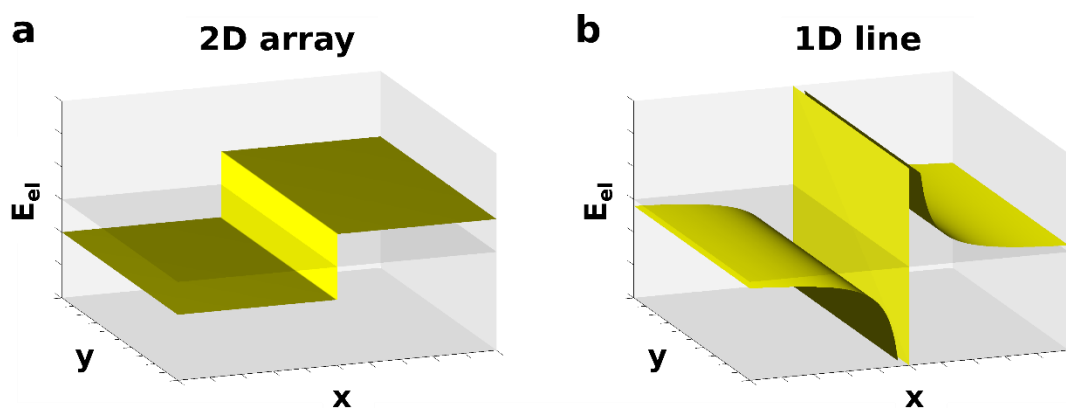


Figure 1. Change in the electrostatic energy of an electron generated by a two-dimensional array and a one-dimensional line of point-dipoles. (a) A two-dimensional array of dipoles (assembled in the yz -plane, at $x=0$, with the dipoles pointing in the x -direction) causes a step in the electrostatic potential (in the $z=0$ plane). (b) A one-dimensional line of dipoles (oriented along the y -direction, at $y=0$, $z=0$, with the dipoles pointing in the x -direction) generates a change in the potential (in the $z=0$ plane) that drops to zero following a $1/r$ decay. Note that the present example is chosen such that inter-dipole distances are negligible compared to the depicted spatial dimensions.

2. General strategy, results, and discussion

2.1. Structures for achieving an electrostatic patterning in graphene

Here, for realizing 1D lines of dipoles in conjunction with graphene, we will rely on two fundamentally different approaches: (i) an in-plane patterning of graphene by direct chemical

embedding of dipole lines, and (ii) an out-of-plane arrangement of dipole lines that can be achieved either via assembling molecules with polar substituents on the graphene sheet or via depositing/growing graphene on substrates containing suitably assembled polar elements. To study the properties of modified graphene sheets, we performed density-functional theory (DFT) based band-structure calculations on suitably chosen supercells (see Methods section for full technical details).

An efficient strategy for localizing states in a certain spatial region without the need of cutting graphene into nanoribbons is arranging two parallel lines of dipoles with opposite dipole orientation at a not too large distance from each other. To investigate the conceptual prospects of such an electrostatic confinement of electronic states through in-plane substitutional dipoles, we rely on systems like the one depicted in **Figure 2a**. There, the most commonly studied substitutional dopands of graphene, namely B and N atoms, are used to create two lines of dipoles with opposite orientation in the graphene plane. Specifically, we chose a symmetric system: graphene stripes with the 14 carbon atoms between the B sides of the dipoles (i.e., in region I in Figure 2) and 14 C atoms between the N sides (i.e., in region II in Figure 2). This results in the unit cell indicated in Figure 2 (additional data for varying thicknesses of the stripes are contained in the Supporting Information, SI). The resulting system is a convenient model for studying the fundamental effects associated with dipole assemblies embedded into graphene^[23]. Furthermore, it can serve as guideline for more realistic out-of-plane dipolar structures embedding (*vide infra*), and has the potential to inspire entirely novel patterning strategies given the tremendous progress that is currently made both in chemically modifying and growing graphene^[24,25] and related nanoribbons^[26,27] in a controlled bottom-up manner.

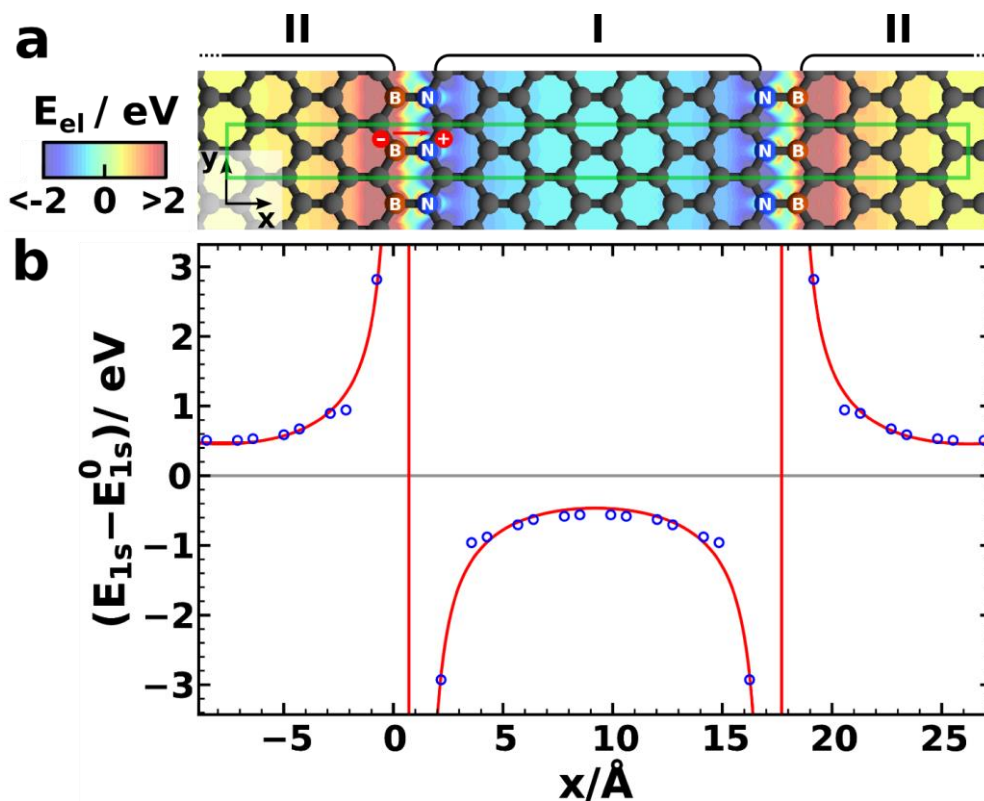


Figure 2. (a) Schematic structure of a prototypical system for in-plane dipole lines by oppositely oriented pairs of substitutional boron (B) and nitrogen (N) atoms in graphene. The green rectangle depicts the unit cell. The plane is colored according to the change in electrostatic energy of an electron when substituting the selected carbon atoms with B and N. (b) Change in C1s core level energies for the carbon atoms depicted in (a) (blue circles; the choice of the energy reference is explained in the Methodology section). The red line is a fit using an electrostatic model (see SI for details).

2.2. Tuning the electrostatic energy

The DFT-calculated effect of dipole lines on the electrostatic energy of an electron in the graphene plane is shown in Figure 2a. It is calculated as the difference of the electrostatic energies of an electron between pristine and BN-substituted graphene (at the fixed geometry of the latter). One can clearly see the lowering of the energy in region I (i.e., between the positive (N) poles of the dipole lines) and a similarly pronounced increase between the

negative (B) poles. This trend is also visible in the associated energies of the C1s core levels of the BN-substituted system (Figure 2b, blue circles) and the plane-averaged electrostatic energy (see SI). Considering the localization of the core states, their relative energies provide an efficient tool for mapping the local electrostatic energy. Consequently, they closely follow the trend for the plane-averaged electrostatic energy as shown in the SI. Only in the immediate neighborhood of the heteroatoms the C1s core-levels certain deviations are found as a consequence of chemical shifts (see SI). Two important conclusions can be drawn from these data: First, the induced modification of the electron electrostatic energy due to the BN dipoles is significant amounting to a decrease of 0.7 eV on average (not taking into account the C-atoms directly bonded to a heteroatom) in region I and an essentially equivalent increase in region II. Secondly, the shift decreases away from the dipoles.

Electrostatically, the effect can be modeled by summing up the fields of point dipoles located at the position of the BN pairs and including an exponential term that accounts for the screening of the potential by the nearly-free electrons in graphene. The excellent agreement of the resulting fit with the actual core level energies (red line in Figure 2, see SI for details) further underlines that the cause of the modified electron energies is electrostatic in nature and not a consequence of the mere change of the local chemical environment by the B and N substituents. The rapid decay of the electrostatic energy away from the BN-lines limits the applicability of the presented patterning approach to comparably narrow graphene stripes with a width of at the most a few nm (about 1.6 nm in the systems shown in Figure 2). Indeed, when studying pairs of BN-lines separated by a large number of C atoms (128 for the example shown in the SI reflecting the situation isolated BN-line pairs), the electrostatic energy quite rapidly drops to that of pure graphene away from the substituents.

2.3. Localizing and energetically shifting electronic states

The shift in the electrostatic energy also has important consequences for the electronic states in the vicinity of the Fermi level (see **Figure 3**). The density of states (DOS, Figure 3a) associated with the area between the dipole lines (region I) shows a shift towards lower energies with respect to unmodified graphene. A shift in the opposite direction is observed for region II. The shifts of the main features of the DOSs compared to pristine graphene amounts to ± 0.7 eV, which is in excellent agreement with the core-level shifts presented above, confirming the electrostatic origin of the discussed effects.

The spatial distribution of the electron density associated with the relevant electronic states can be examined by means of a map of the local density of states (LDOS, see Methods section for details) in Figure 3b (for a 3D representation of that plot see TOC graphics). Clearly, the states in regions I and II between the dipole lines are energetically shifted with respect to each other: The unoccupied states close to the Fermi level are mainly localized inside region I. Conversely, the DOS of occupied states in that region is comparably low. Pronounced intensities of occupied states are found either close to the B-ends of the stripes, or localized directly on the B-atoms (which is typical for B-doping of graphene^[11,28]). This indicates that the occupied and the unoccupied states around the Fermi level are indeed largely localized in different regions of the system. In contrast to the situation often found in graphene nanoribbons^[29-31], these electronic levels are not spin-polarized edge states. We note that impurities in the sample may lead to changes of the DOS and shifts of the Fermi-level, which changes the screening and, hence, can couple to the electrostatic effects. Furthermore, we also note that the electrostatic fields stemming from a gate electrode can also be used for localizing and guiding electrons in graphene^[32,33].

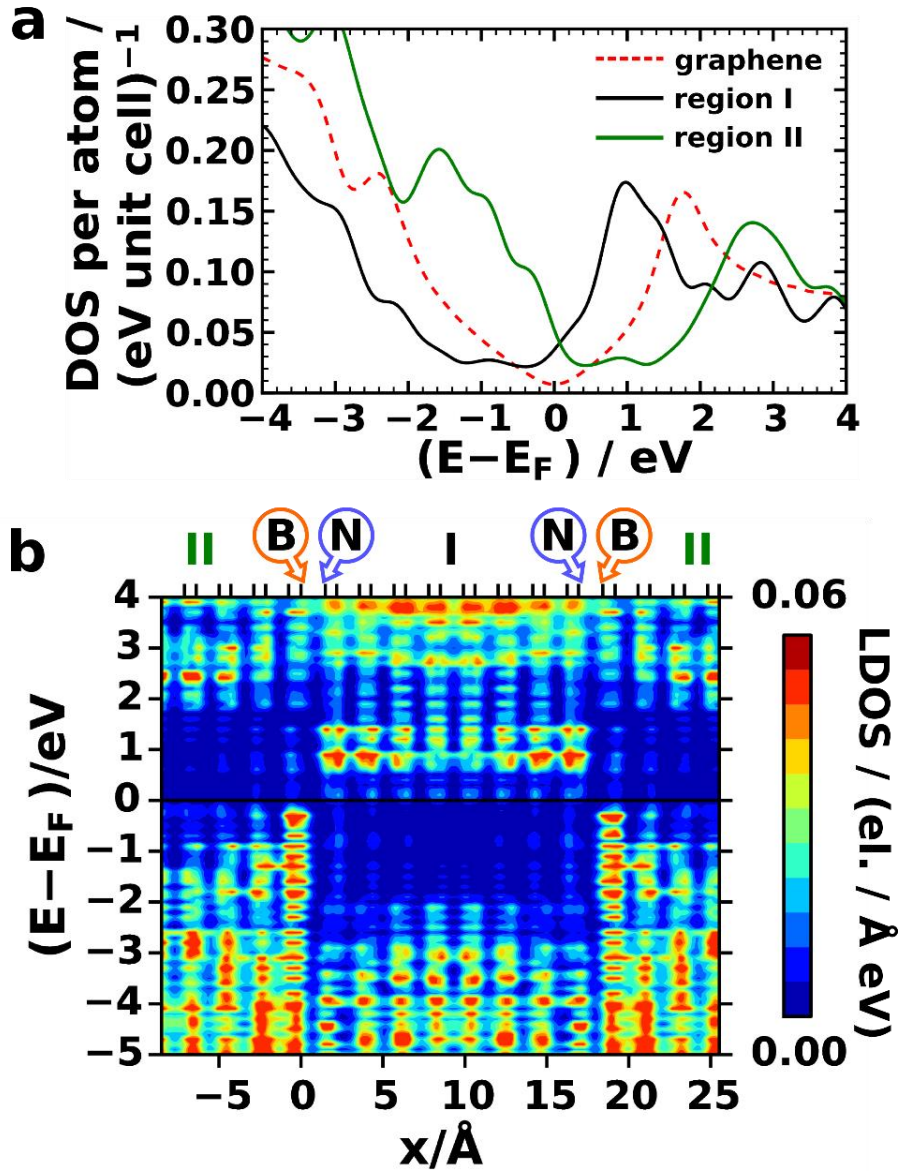


Figure 3. (a) Density of states of pure graphene (dashed red line), and projection of the density of states of a BN pair substituted graphene sheet onto the region between the two dipole lines. The black line corresponds to the projection onto region I in (b) (with lowered electrostatic energy) and the green line corresponds to region II (with increased electrostatic energy). (b) Color-coded LDOS integrated over y, z , see methods section for details. The x -positions of the individual atoms are indicated as ticks at the top axis of the plot, where all the ticks correspond to C-atoms apart from the explicitly marked BN pairs. The two regions introduced in Figure 2 are marked here as I and II. Note that the occupied states are mainly located between the B atoms and the unoccupied states between the N atoms.

As graphene is a semimetal any confinement of occupied and unoccupied frontier-states to certain spatial regions naturally cannot be complete^[32]. Due to the absence of a band-gap there will always be occupied as well as unoccupied states right above and below E_F in all regions of space, even if their densities vary significantly. An interesting aspect in this context is that, as shown in Figure 3a, the DOS at E_F increases significantly compared to pristine graphene between the pairs of the BN-lines, both in region I and region II. The main reason for that is that in pristine graphene the DOS directly at E_F is minimal^[34] and, consequently, any energetic shifting of the states yields an increase of $DOS(E_F)$. In passing we mention that in the present case changes in the shape of the band-structure also impact the DOS (vide infra). The increase of $DOS(E_F)$ due to a local shifting of the energy levels implies that the likelihood of finding charge carriers (electrons as well as holes) injected into BN-patterned graphene sheet should be highest in the vicinity of the dipole lines.

An alternative view on the localization of individual states can be gained by investigating the band structure of BN-modified graphene (see **Figure 4a**). In the hexagonal Brillouin zone of pure graphene the Dirac cone with its linear dispersion relation around the Fermi level is located at the K-point^[34]. For the rectangular unit-cell studied here this feature appears between the Γ and the Y point^[35] (c.f., band-structure of unmodified graphene plotted as black line in Figure 4a). In the following, this k-point will be denoted as ‘K’. When introducing opposing lines of BN groups, the linear dispersion around E_F is lost and the bands adopt a more parabolic shape, reminiscent to what is observed for bilayer graphene^[36–38]. In the present system this can be associated with viewing the band-structure of BN-modified graphene as a superposition of energetically shifted graphene band structures, as discussed below.

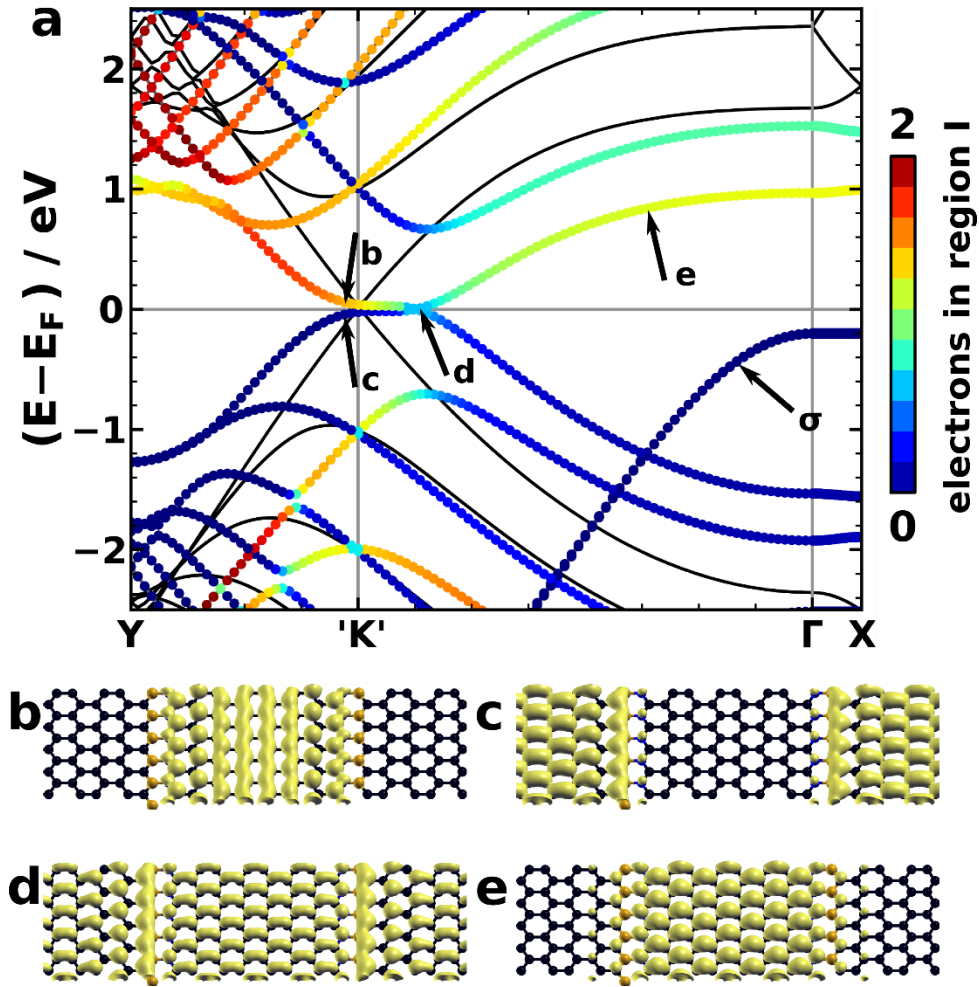


Figure 4. (a) Kohn-Sham band structure of graphene in a rectangular unit cell (black lines) and graphene modified by opposing lines of BN pairs (colored points). The X-direction in the rectangular first Brillouin zone corresponds to the direction perpendicular to the dipole lines (parallel to the dipole moments), the Y-direction is the direction along the dipole lines; the K-point of the hexagonal Brillouin zone is now found between Γ and Y and denoted by 'K'. Each state is color-coded according to its weight in region I between the BN-lines. Dark-red shading means complete localization in region I, dark-blue shading corresponds to no weight of the states in that region. For (nearly) degenerate bands, the two values are averaged, which leads to “blurred” values at the points where bands are crossing. The band marked by σ has predominantly sigma character and the states are localized largely on the B and N atoms (see correspondingly color-coded band structure in the SI). (b-e) Isosurface plots of the electron density (isovalued 0.01 electron/Å³) for the states marked accordingly in the band

structure (a). Region I is centered in these plots. Similar plots for other states can be found in the SI.

To identify the localization of each state in the band-structure, each plotted point is color coded according to the extent to which the corresponding state is localized either in region I between the BN-lines (see Figure 4a), in region II, or directly on the B and N atoms (for the latter two plots see SI). Again, one clearly sees that the unoccupied states near the Fermi level are mostly localized in region I, the unoccupied states are localized in region II (see corresponding plot in the SI). The σ -band indicated in Figure 4a is localized on the B and N atoms. For two selected states near the Fermi level, iso-density plots are shown in Figures 4c and d fully confirming the localization of the states. The inclusion of dipolar lines into graphene indeed allows localizing individual Bloch-states in different areas of the unit cell.

Interestingly, the degree of localization of the electronic states not only changes from band to band but also within a band as a function of the k-vector. For example, the electron density of the frontier band containing the states displayed in Figure 4c, d and e changes localization when cutting through the Fermi-energy. Such a change of localization, albeit in the opposite direction, is also observed for the second frontier band of π -character. Notably, the states directly at E_F remain essentially delocalized (cf., state in Figure 4d) and the largest degree of localization is found between 'K' and Y.

Another interesting aspect of the band-structure of BN-modified graphene is that the majority of its features can be at least qualitatively reproduced by a superposition of an artificially upwards- and a downwards-shifted graphene band-structure, as shown in **Figure 5**. Comparing Figure 4a and 5 one sees that the features associated with the upwards-shifted band-structure are localized in region II and the downward-shifted features in region I,

supporting the notion that the observed modifications of the band-structure are primarily electrostatic in nature. The only qualitative deviations between the band structure of the BN substituted system and the superposition of the shifted graphene band structures occur (i) for the σ -band (which is localized on the B and N atoms), (ii) in the region, where the bands of the combined system cross E_F and (iii) between the Γ and X points. (ii) is associated with the fact that the states immediately at E_F are delocalized over the whole unit cell (see Figure 4d). The only weakly dispersing bands in the Γ -X direction in BN-substituted graphene are a direct consequence of the localization of the states (preventing efficient coupling between neighboring unit cells).

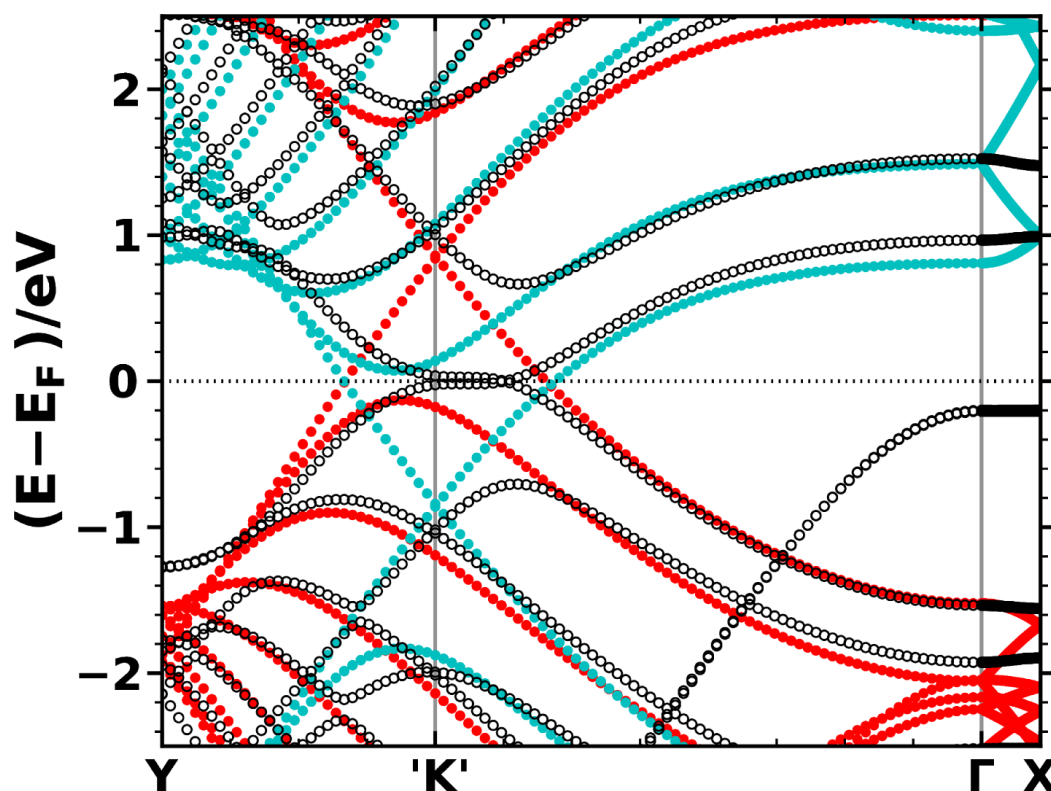


Figure 5. Band structure of BN-modified graphene (black circles) together with the band structure of pure graphene in a rectangular unit cell, shifted up and down in energy by 0.85 eV (red and cyan points).

2.4. Electrostatic patterning via the adsorption of polar molecules

The compound with in-plane substitutions discussed so far serves as an ideal proof-of-principle system to demonstrate the conceptual consequences of dipole patterning of graphene. Out-of-plane approaches, however, appear more feasible experimentally. As an example for such an out-of-plane electrostatic patterning, we studied the modification of graphene by regular adsorption of dicyano-substituted diphenylacetylene molecules as shown in **Figure 6a**. Note that the cyano end-groups create oppositely oriented lines of local dipoles in the spirit of the BN dipoles discussed above.

Analogous to the dipole lines in BN-substituted graphene, the adsorbed line of (quadrupolar) molecules locally changes the electrostatic potential within the graphene sheet (see Figure 6a). This also results in a shift of the energy of the individual states, which becomes apparent in the shift of the projected DOS curves plotted in Figure 6b. The energies of the electronic states in the graphene strip underneath the molecules and, thus, between the dipole lines (in region I) are lowered; the ones of states further away from the molecule (in region II) increased. The effect is, however, comparably small with the shift between the regions I and II amounting to ~ 0.2 eV. This can be explained (i) by a reduced dipole density and (ii) the lateral distance of the dipoles from the graphene sheet and the associated drop of the electric field. This distance corresponds to the adsorption height of the molecules, which was calculated to be 3.34 \AA . The influence of charge transfer plays a minor role for this effect (as the net charge transfer between graphene and the adsorbate amounts to ~ 0.05 electrons per adsorbate molecule, see SI) and again the shift of the states due to a change of the electrostatic energy as a result of the superposition of the dipole fields dominates.

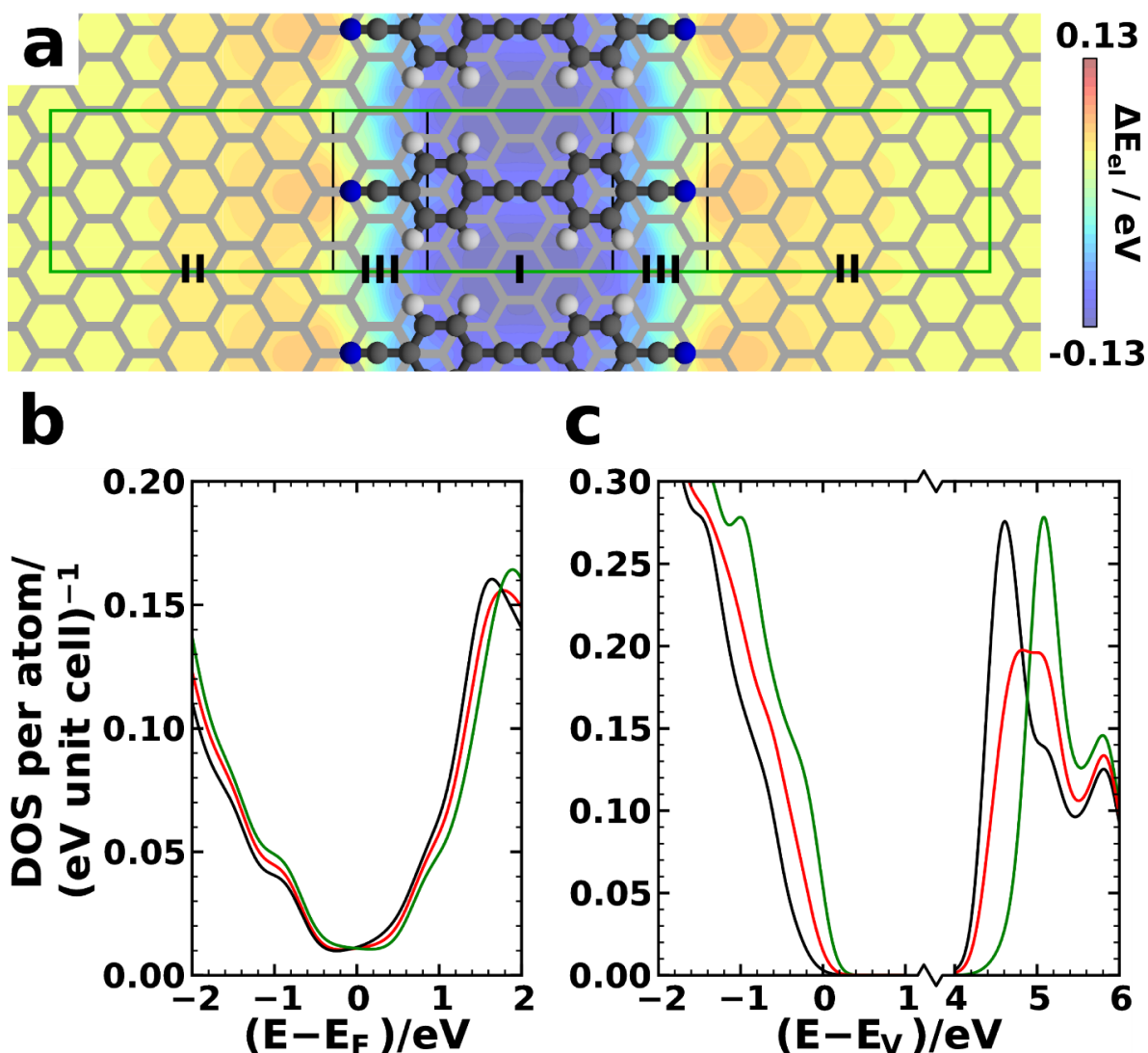


Figure 6. (a) Structure of a dicyano-substituted diphenylacetylene molecule adsorbed on graphene (mean adsorption height 3.34\AA). The unit cell is shown as a green rectangle and divided into three regions I, II and III. The change of electrostatic energy of an electron in the graphene plane upon adsorption of the molecule is shown as well. (b) Density of states projected onto the atoms in the regions I (black line), II (green line) and III (red line) of the graphene sheet in this system. (c) Density of states of hexagonal boron nitride (hBN) in the same geometry as graphene with an adsorbed dicyano-substituted diphenylacetylene molecule. The DOS is projected onto the atoms in the three regions of the hBN sheet. The energy is given relative to the valence band edge E_V . Note that the energy axes of plots (b) and (c) are on the same scale.

2.5. Expanding the electrostatic patterning concept to hexagonal boron nitride

The above results imply that for 2D materials with smaller dielectric constants that less efficiently screen the field of the dipoles, a stronger effect is to be expected. Indeed, the shift of the band-edges in hexagonal boron nitride (hBN) upon adsorbing the dicyano-substituted diphenylacetylenes is much larger (~ 0.6 eV, as shown in Figure 6c). This renders the out of plane patterning approach particularly promising for less polarizable systems such as layered semiconductors.

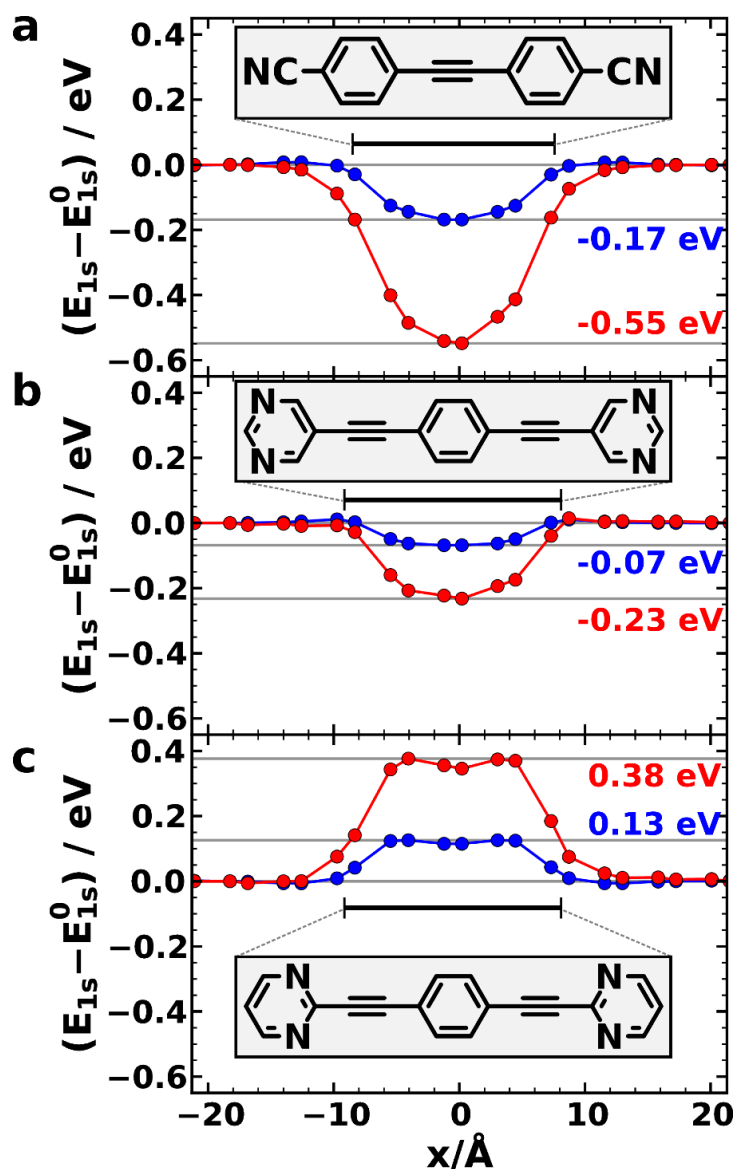


Figure 7. Electrostatic energy of an electron determined via the core-level shifts of the 1s electrons in graphene (blue circles) and hBN (red circles) due to the adsorption of the

quadrupolar molecules shown in the insets (only core levels for atoms at $y=0$ are shown). The horizontal black bars represent the size and position of the molecules (not taking into account H-atoms).

The magnitude and direction of the shift in the electrostatic energy is crucially impacted by the magnitude and direction of the dipole moment of the end groups (i.e., the quadrupole moment of the whole molecule), as shown in **Figure 7**. There, the impact of the molecule already presented in Figure 6 is compared to two pyrimidine-terminated systems. An interesting aspect of the latter molecules is that, by changing the position of the N atoms in the outer rings, the local dipole moments can be reversed^[39]. Consequently, the electrostatic energy below the molecule is raised for a molecule with outward-pointing dipole moments (Figure 7c), as opposed to the lowering of the electrostatic energy observed for molecules with inward-pointing dipoles (Figure 7a and b). Consistent with the findings of Figure 6, the effect of adsorbed molecules on hBN is more than twice as high as on graphene due to the reduced screening in hBN.

Finally, we would like to comment on strategies for an experimental implementation of our findings: One can envision to realize polar patterns in practice via a self-assembly of molecules bearing polar substituents, whose arrangement is stabilized through hydrogen bonds or direct chemical links^[40,41]. Alternatively, a bottom-up synthesis^[10–14] of nanoribbons bearing polar peripheral substituents to be deposited onto the graphene is also conceivable. Also a top-down patterning of a substrate followed by the (self)assembly of polar molecules and a subsequent deposition of a graphene sheet is appears as an interesting possibility. Indeed, our initial attempts leave significant room for improvements towards an optimized out of plane electrostatic patterning involving an ideal combination of dipole density, chemical stability, and dielectric screening in the 2D material.

3. Conclusions and outlook

In summary, an approach for efficiently tuning the electronic structure of layered systems by exploiting collective electrostatic effects is developed using DFT calculations. We show that the regular 1D assembly of polar units within or above the plane of graphene (as a prototypical 2D system) results in a localization of the electronic states in specific spatial regions. Concomitant with that, a shift of the energetic positions of the localized states relative to the Fermi-level is observed (visible both in the density of states as well as in the band structure). The purely electrostatic origin of this state localization and energetic tuning implies that the suggested strategy offers a quite general way for controlling the electronic properties of 2D materials. This assessment is supported by calculations on electrostatically patterned hexagonal boron nitride.

Considering that in practice the necessary assemblies of polar elements can be achieved exploiting the wide range of molecular self-assembly processes, one can envision also a much more complex “shaping” of electronic states in 2D materials compared to the relatively straightforward confinement in linear structures presented here. Deviating from highly symmetric arrangements of dipoles could well lead to interesting new effects triggered, for example, by local variations of the electric fields at the corners of kinked polar lines occurring on top of the collective effects discussed here. Beyond that, it will be interesting to study, how the above described effects work out in multilayer systems including van der Waals bonded homo- and heterostructures and multilayer graphene.

4. Methods

The simulations were carried out applying density functional theory using the Vienna Ab-Initio Simulation Package (VASP)^[42–45] 5.3.3 and the PBE^[46,47] functional. Soft PAW^[48,49]

pseudopotentials and a plane-wave cutoff energy of 279.692 eV were employed. The Brillouin zone was sampled with a Gamma-centered Monkhost-Pack^[50] k-point grid, which was checked for numerical convergence for a simple graphene unit cell (converged grid: 21x21x1) and then scaled down according to the supercell size (6x21x1 for the BN-substituted graphene systems investigated here, 1x21x1 for the systems with adsorbed molecules). The Gaussian smearing occupation scheme with SIGMA=0.01 eV (this corresponds to a standard deviation of $0.01/\sqrt{2}$ eV) was used. The density of states was then calculated using a Gaussian broadening with a standard deviation of $0.3/\sqrt{2}$ eV.

Core level shifts were calculated in the initial state approximation,^[51] as implemented in VASP^[52]. This is useful, as the core-level energies are used here to map trends in the electrostatic energy rather than to quantitatively predict x-ray core level spectra. For the latter, approaches including core-hole screening effects would potentially be necessary, which may, however, obscure the purely electrostatic shifts we are interested in here. Note that the energy reference for the C1s core levels in Figure 2b was determined by averaging over the C1s core levels of the four C-atoms furthest away from, and thus least affected by, the dipole lines. Changes in the electrostatic energy upon introducing dipolar elements are calculated by subtracting the electrostatic energy of a single graphene sheet from the electrostatic energy of the total system including the elements, both aligned relative to the vacuum level below the sheet.

The local density of states (LDOS) shown in Figure 3b is defined as the electron density corresponding to specific energy intervals (with energy resolution 0.1 eV). The LDOS is a function that thus depends both on the spatial position and on the energy. Integrating it along the y- and z-axis, one obtains the quantity shown in Figure 3b. This quantity is a measure for the DOS, both as a function of energy and of the spatial position in the direction perpendicular

to the dipolar lines. To obtain the color-coded information shown in Figure 4a, the k -resolved band-projected charge density was calculated for each state in the band structure and then integrated spatially in region. The iso-electron-density plots in Figure 4b to e were created using XCrysDen^[53]; for obtaining the other figures the Python libraries Numpy^[54] and Matplotlib^[55] were used.

For simulating 2D-periodic systems in a 3D-periodic code, the slab approach with a vacuum gap of 20 Å was used (this value is sufficient for avoiding stray-fields from periodic replicas of graphene as shown in the SI). The geometries of the individual systems were optimized using the GADGET tool^[56] until the remaining forces on the ions were smaller than 0.01 eV/Å. For systems that included adsorbed molecules, the graphene geometry was held fixed and only the atoms belonging to the molecule were allowed to move. For these calculations, van der Waals forces play an important role and, therefore, were taken into account in our calculations using the pair-wise vdW-TS^[57] scheme. The particular choice of the starting geometry does impact the final structure of the molecules adsorbed on graphene, but that does not have a significant impact on the observed effects, as shown in the SI. Also note that when determining the electronic structure of the studied systems, the positions of the nuclei have been fixed; i.e., bearing in mind also the very small smearing used for the occupation of the electronic states, a quasi-static low-temperature situation is modelled. This neglects disorder induced by thermal motion, but as long as the thermal fluctuations do not destroy the arrangement of the molecules used when patterning via adsorption of polar molecules, this will have no qualitative impact on the results discussed here.

Supporting Information

Supporting Information is available from the Wiley Online Library or from the author.

Acknowledgements

The authors thank Emanuel Lörtscher for stimulating discussions. Financial support by the Austrian Science Fund (FWF): I937-N19 within the ERA-Chemistry framework is gratefully acknowledged. The computational studies presented have been performed using the clusters of the division for high-performance computing at the Graz University of Technology.

Received: ((will be filled in by the editorial staff))

Revised: ((will be filled in by the editorial staff))

Published online: ((will be filled in by the editorial staff))

- [1] A. K. Geim, K. S. Novoselov, *Nat. Mater.* **2007**, *6*, 183.
- [2] M. H. Rummeli, C. G. Rocha, F. Ortmann, I. Ibrahim, H. Sevincli, F. Börrnert, J. Kunstmann, A. Bachmatiuk, M. Pötschke, M. Shiraishi, M. Meyyappan, B. Büchner, S. Roche, G. Cuniberti, *Adv. Mater.* **2011**, *23*, 4471.
- [3] K. Kim, J.-Y. Choi, T. Kim, S.-H. Cho, H.-J. Chung, *Nature* **2011**, *479*, 338.
- [4] T. Otsuji, S. A. Boubanga Tombet, A. Satou, H. Fukidome, M. Suemitsu, E. Sano, V. Popov, M. Ryzhii, V. Ryzhii, *J. Phys. Appl. Phys.* **2012**, *45*, 303001.
- [5] Y. Wu, K. A. Jenkins, A. Valdes-Garcia, D. B. Farmer, Y. Zhu, A. A. Bol, C. Dimitrakopoulos, W. Zhu, F. Xia, P. Avouris, Y.-M. Lin, *Nano Lett.* **2012**, *12*, 3062.
- [6] W. Fu, M. El Abbassi, T. Hasler, M. Jung, M. Steinacher, M. Calame, C. Schönenberger, G. Puebla-Hellmann, S. Hellmüller, T. Ihn, A. Wallraff, *Appl. Phys. Lett.* **2014**, *104*, 013102.
- [7] Y.-M. Lin, A. Valdes-Garcia, S.-J. Han, D. B. Farmer, I. Meric, Y. Sun, Y. Wu, C. Dimitrakopoulos, A. Grill, P. Avouris, K. A. Jenkins, *Science* **2011**, *332*, 1294.
- [8] L. Britnell, R. V. Gorbachev, R. Jalil, B. D. Belle, F. Schedin, A. Mishchenko, T. Georgiou, M. I. Katsnelson, L. Eaves, S. V. Morozov, N. M. R. Peres, J. Leist, A. K. Geim, K. S. Novoselov, L. A. Ponomarenko, *Science* **2012**, *335*, 947.
- [9] T. Roy, M. Tosun, J. S. Kang, A. B. Sachid, S. B. Desai, M. Hettick, C. C. Hu, A. Javey, *ACS Nano* **2014**, *8*, 6259.

- [10] L. S. Panchakarla, K. S. Subrahmanyam, S. K. Saha, A. Govindaraj, H. R. Krishnamurthy, U. V. Waghmare, C. N. R. Rao, *Adv. Mater.* **2009**, NA.
- [11] L. Zhao, M. Levendorf, S. Goncher, T. Schiros, L. Pálová, A. Zabet-Khosousi, K. T. Rim, C. Gutiérrez, D. Nordlund, C. Jaye, M. Hybertsen, D. Reichman, G. W. Flynn, J. Park, A. N. Pasupathy, *Nano Lett.* **2013**, *13*, 4659.
- [12] D. Wei, Y. Liu, Y. Wang, H. Zhang, L. Huang, G. Yu, *Nano Lett.* **2009**, *9*, 1752.
- [13] Y. Wang, Y. Shao, D. W. Matson, J. Li, Y. Lin, *ACS Nano* **2010**, *4*, 1790.
- [14] K. Brenner, R. Murali, *Appl. Phys. Lett.* **2011**, *98*, 113115.
- [15] H. J. Xiang, B. Huang, Z. Y. Li, S.-H. Wei, J. L. Yang, X. G. Gong, *Phys. Rev. X* **2012**, *2*, 011003.
- [16] J. Zhou, M. M. Wu, X. Zhou, Q. Sun, *Appl. Phys. Lett.* **2009**, *95*, 103108.
- [17] R. R. Nair, W. Ren, R. Jalil, I. Riaz, V. G. Kravets, L. Britnell, P. Blake, F. Schedin, A. S. Mayorov, S. Yuan, M. I. Katsnelson, H.-M. Cheng, W. Strupinski, L. G. Bulusheva, A. V. Okotrub, I. V. Grigorieva, A. N. Grigorenko, K. S. Novoselov, A. K. Geim, *Small* **2010**, *6*, 2877.
- [18] K. S. Novoselov, V. I. Fal'ko, L. Colombo, P. R. Gellert, M. G. Schwab, K. Kim, *Nature* **2012**, *490*, 192.
- [19] O. L. A. Monti, *J. Phys. Chem. Lett.* **2012**, *3*, 2342.
- [20] A. Natan, L. Kronik, H. Haick, R. T. Tung, *Adv. Mater.* **2007**, *19*, 4103.
- [21] G. Heimel, F. Rissner, E. Zojer, *Adv. Mater.* **2010**, *22*, 2494.
- [22] B. Kretz, D. A. Egger, E. Zojer, *Adv. Sci.* **2015**, *2*, 1400016.
- [23] Note that a growth of phase-separated domains of graphene and h-BN in the same lattice plane comprising lattice matched edges has indeed been observed, described in L. Ci, L. Song, C. Jin, D. Jariwala, D. Wu, Y. Li, A. Srivastava, Z. F. Wang, K. Storr, L. Balicas, F. Liu, and P. M. Ajayan, *Nat. Mater.* **2010**, *9*, 430.
- [24] D. Wei, Y. Liu, *Adv. Mater.* **2010**, *22*, 3225.

- [25] L. Chen, Y. Hernandez, X. Feng, K. Müllen, *Angew. Chem. Int. Ed.* **2012**, *51*, 7640.
- [26] J. Cai, P. Ruffieux, R. Jaafar, M. Bieri, T. Braun, S. Blankenburg, M. Muoth, A. P. Seitsonen, M. Saleh, X. Feng, K. Müllen, R. Fasel, *Nature* **2010**, *466*, 470.
- [27] A. Narita, X. Feng, Y. Hernandez, S. A. Jensen, M. Bonn, H. Yang, I. A. Verzhbitskiy, C. Casiraghi, M. R. Hansen, A. H. R. Koch, G. Fytas, O. Ivasenko, B. Li, K. S. Mali, T. Balandina, S. Mahesh, S. De Feyter, K. Müllen, *Nat. Chem.* **2013**, *6*, 126.
- [28] L. Zhao, R. He, K. T. Rim, T. Schiros, K. S. Kim, H. Zhou, C. Gutierrez, S. P. Chockalingam, C. J. Arguello, L. Palova, D. Nordlund, M. S. Hybertsen, D. R. Reichman, T. F. Heinz, P. Kim, A. Pinczuk, G. W. Flynn, A. N. Pasupathy, *Science* **2011**, *333*, 999.
- [29] K. Nakada, M. Fujita, G. Dresselhaus, M. S. Dresselhaus, *Phys. Rev. B* **1996**, *54*, 17954.
- [30] Y.-W. Son, M. L. Cohen, S. G. Louie, *Nature* **2006**, *444*, 347.
- [31] C. Tao, L. Jiao, O. V. Yazyev, Y.-C. Chen, J. Feng, X. Zhang, R. B. Capaz, J. M. Tour, A. Zettl, S. G. Louie, H. Dai, M. F. Crommie, *Nat. Phys.* **2011**, *7*, 616.
- [32] R. R. Hartmann, N. J. Robinson, M. E. Portnoi, *Phys. Rev. B* **2010**, *81*, 245431.
- [33] J. R. Williams, T. Low, M. S. Lundstrom, C. M. Marcus, *Nat. Nanotechnol.* **2011**, *6*, 222.
- [34] A. H. Castro Neto, N. M. R. Peres, K. S. Novoselov, A. K. Geim, *Rev. Mod. Phys.* **2009**, *81*, 109.
- [35] The lattice vectors (both in real and reciprocal space) for pure graphene in the rectangular unit cell slightly differ from the equivalent BN-substituted system (due to the geometry optimization). In all band structure plots, the k-axes were rescaled so that the Gamma, X and Y points of all systems coincide.
- [36] S. Trickey, F. Müller-Plathe, G. Dierksen, J. Boettger, *Phys. Rev. B* **1992**, *45*, 4460.
- [37] T. Ohta, *Science* **2006**, *313*, 951.
- [38] M. Aoki, H. Amawashi, *Solid State Commun.* **2007**, *142*, 123.

- [39] D. A. Egger, F. Rissner, E. Zojer, G. Heimel, *Adv. Mater.* **2012**, *24*, 4403.
- [40] J. V. Barth, G. Costantini, K. Kern, *Nature* **2005**, *437*, 671.
- [41] L. Grill, M. Dyer, L. Lafferentz, M. Persson, M. V. Peters, S. Hecht, *Nat. Nanotechnol.* **2007**, *2*, 687.
- [42] G. Kresse, J. Hafner, *Phys. Rev. B* **1993**, *47*, 558.
- [43] G. Kresse, J. Hafner, *Phys. Rev. B* **1994**, *49*, 14251.
- [44] G. Kresse, J. Furthmüller, *Comput. Mater. Sci.* **1996**, *6*, 15.
- [45] G. Kresse, J. Furthmüller, *Phys. Rev. B* **1996**, *54*, 11169.
- [46] J. P. Perdew, K. Burke, M. Ernzerhof, *Phys. Rev. Lett.* **1996**, *77*, 3865.
- [47] J. P. Perdew, K. Burke, M. Ernzerhof, *Phys. Rev. Lett.* **1997**, *78*, 1396.
- [48] P. E. Blöchl, *Phys. Rev. B* **1994**, *50*, 17953.
- [49] G. Kresse, D. Joubert, *Phys. Rev. B* **1999**, *59*, 1758.
- [50] H. J. Monkhorst, J. D. Pack, *Phys. Rev. B* **1976**, *13*, 5188.
- [51] M. Methfessel, D. Hennig, M. Scheffler, *Surf. Sci.* **1993**, 287-288, 785.
- [52] L. Köhler, G. Kresse, *Phys. Rev. B* **2004**, *70*, 165405.
- [53] A. Kokalj, *Comput. Mater. Sci.* **2003**, *28*, 155.
- [54] S. van der Walt, S. C. Colbert, G. Varoquaux, *Comput. Sci. Eng.* **2011**, *13*, 22.
- [55] J. D. Hunter, *Comput. Sci. Eng.* **2007**, *9*, 90.
- [56] T. Bučko, J. Hafner, J. G. Ángyán, *J. Chem. Phys.* **2005**, *122*, 124508.
- [57] A. Tkatchenko, M. Scheffler, *Phys. Rev. Lett.* **2009**, *102*, 073005.

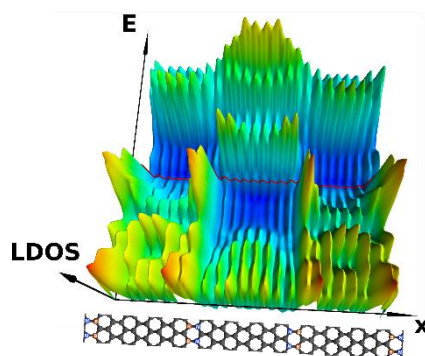
The table of contents entry

Collective electrostatic effects stemming from dipole lines are shown to locally manipulate the electronic properties of 2D materials (graphene and the insulating hexagonal boron nitride). This can be used to shift the individual states of the material and to localize them in regions around the dipoles.

Keywords: graphene; 2D materials; DFT calculations; collective electrostatic effects; orbital localization

Gernot J. Kraberger, David A. Egger, Egbert Zojer*

Tuning the electronic structure of graphene through collective electrostatic effects



TOC graphics: Spatially resolved density of states of graphene modified by BN-double-lines (for their position along the x-axis, see the unit cell plot at the bottom). These are the same data as in Figure 3, with the local density of states (LDOS) plotted along a third axis to be able to see the relative height of the peaks. The energy axis goes from -5 to 4 eV around the Fermi level, which is marked by a red horizontal line.